Emergence of visible light optical properties of L-phenylalanine aggregates

Mantas Ziaunys, Vytautas Smirnovas

Institute of Biotechnology, Life Sciences Center, Vilnius University, Vilnius, Lithuania

Corresponding Author:
Vytautas Smirnovas
Sauletekio al. 7, Vilnius, LT-10257, Lithuania

Email address: vytautas.smirnovas@bti.vu.lt

Abstract

The ability of phenylalanine to form fibrillar nanostructures was demonstrated on multiple occasions and such an oligomerization reaction could be the cause of cytotoxicity in patients with phenylketonuria. These findings were supported by claims that L-phenylalanine (Phe) fibrils have amyloid properties and can be detected using thioflavin T (ThT) fluorescence assay. However, a part of Phe aggregation studies reported the opposite data, suggesting no amyloid structures to be formed. Due to the contradicting reports, the amyloid nature of Phe aggregates remains uncertain. In this work we tested Phe aggregation under conditions where amyloid formation was previously reported. We show the emergence of Phe aggregates with visible light optical properties that overlap with the spectra of dyes used in amyloid fibril assays, which could lead to false-positive identifications.

Introduction

Amyloid fibrils are linked to several neurodegenerative disorders, such as Alzheimer's or Parkinson's disease (Chiti & Dobson, 2006) and their formation is the result of protein aggregation into highly ordered structures (Fitzpatrick et al., 2013). It was shown that full length amyloid proteins are not required for such aggregation to occur(Halverson et al., 1990; von Bergen et al., 2000). In order to find the minimum possible peptide capable of fibril formation, shorter and shorter fragments were tested, all the way down to dipeptides (Azriel & Gazit, 2001; Reches & Gazit, 2003; Gazit, 2007). Eventually it was demonstrated by Adler-Abramovich *et al.* that even unmodified monomeric Phe is capable of forming fibrillar aggregates(Adler-Abramovich et al., 2012), which share similarities to amyloids. The amyloidogenic nature of Phe fibrils were supported by experimental data, showing the presence of beta-sheet conformation (by CD)(Smith et al., 2008), and other amyloid-specific properties, such as ThT and Congo Red

40 binding ability and even seeding potential(Singh et al., 2014; Shaham-Niv et al., 2015; Anand et
41 al., 2017). Different models of aggregate assembly and structure types were also
42 presented.(Mossou et al., 2014; German, Uyaver & Hansmann, 2015; Do, Kincannon & Bowers,
43 2015) However, later Perween *et al.* suggested that the CD spectra may be interpreted by
44 carboxyl group (n-π*) and benzene ring (π-π*) transitions and was not the result of amyloid
45 assemblies(Perween et al., 2013). It was also shown that these fibrils only form at the edges of
46 confocal microscopy samples due to crystallization(Perween et al., 2013) and that they do not
47 exist in solution(Griffith et al., 2015). The conditions used to generate these fibrils were varied,
48 with some using low concentrations of Phe and others creating supersaturated hydrogels(Adler-
49 Abramovich et al., 2012; Perween et al., 2013; Singh et al., 2014; Shaham-Niv et al., 2015; De
50 Luigi et al., 2015; Banik et al., 2016, 2017).
51 ThT fluorescence was the major assay to confirm Phe amyloid fibril formation, however, the
52 possibility of a false positive detection was not considered. Hydrogel formation could
53 immobilize ThT and increase its fluorescence potential(Hutter et al., 2011) in a similar way as
54 binding to amyloids would, so it should be considered in case of aggregation studies at high Phe
55 concentrations. Autofluorescence of Phe aggregates is another factor to be considered.
56 Previously reported Phe aggregation models display π-stacking as a large contributor to stable
57 aggregate formation(Gazit, 2002; Mossou et al., 2014; German, Uyaver & Hansmann, 2015; Do,
58 Kincannon & Bowers, 2015). π-stacking has been reported to create optically active
59 aggregates(Kuo, 2011; Handelman et al., 2016) and is responsible for large red-shifts of
60 fluorescence emissions through the formation of J-aggregates(McRae & Kasha, 1958; Higgins &
61 Barbara, 1995; Uemori et al., 2012; Cao et al., 2014), which could overlap with amyloid-bound
62 dye fluorescence. In this work we generated Phe aggregates using previously described methods
63 and analyzed their spectroscopic profiles in order to determine whether they interacted with ThT
64 or formed π-stacking optically active structures.

65

Materials & Methods

67 **Phenylalanine sample preparation**

68

69 100 mM Phe samples were prepared by dissolving Phe in 50 mM (pH 6) phosphate buffer at 25°
70 C. Phe aggregation was carried out at 60° C with no sample agitation for 15 days.

71

72 **Fluorescence measurements**

73

74 Solution fluorescence spectra were recorded using an excitation range of 200-500 nm, emission
75 range of 250-650 nm and wavelength increment of 5 nm, with excitation slit - 5 nm, emission slit
76 - 5 nm for incubation observations and excitation slit - 10 nm, emission slit - 5 nm for final
77 aggregate solution analysis with a Varian Cary Eclipse spectrophotometer. Each spectrum was
78 averaged from 3 separate measurements with subtracted 50 mM pH 6 phosphate buffer spectra.

79

80 **Aggregate filtration and sonication**
81
82 Regenerated cellulose filters (0.22 μm) and Amicon concentrators (3 kDa) were used to remove
83 different size of aggregates. Sonication of aggregates was performed using Bandelin Sonopuls
84 3100 sonicator equipped with a MS72 tip for 20 s at 20 % intensity.
85
86 **Hydrogel preparation**
87
88 Hydrogels were prepared by heating a 50 mM (pH 6) phosphate buffer to 100 °C and dissolving
89 agarose to a concentration of 1% or L-phenylalanine to a concentration of 300 mM and adding
90 ThT to a concentration of 50 μM. ThT fluorescence was measured before (at 80 °C) and after (at
91 25 °C) hydrogel formation using 440 nm wavelength excitation and 470-510 nm emission range
92 with excitation slit - 10 nm, emission slit - 5 nm. Each spectrum was averaged from 3 separate
93 measurements.
94
95 **ThT sample spectra measurements**
96
97 1 μL of 10 mM ThT solution was added to 199 μL of 100 mM Phe aggregate solution, to a final
98 ThT concentration of 50 μM. The 3D spectra were measured using the previously described
99 method.
100

Results and discussion

102 100 mM Phe samples were incubated at 60° C and their excitation/emission spectra were
103 measured every 3 days (Figure 1). The initial samples with no incubation only contained Phe-
104 specific emissions (Figure 1A). After 3 days of incubation, a large region of low intensity
105 fluorescence emission appeared on both near-UV and visible light spectrum (Figure 1B). Such
106 emissions were also seen by Tikhonova et al. at lower Phe concentrations and attributed to deep-
107 blue autofluorescence from amino acid oxidation (Tikhonova et al., 2018). Continuous
108 incubation lead to an increasing intensity of these emissions and further expansion into longer
109 wavelength regions (Figures 1C-F). There was also a noticeable decrease in Phe-specific
110 fluorescence emission intensities. After 12 days of incubation, the spectra no longer experienced
111 any substantial changes upon further incubation. The newly formed fluorescence
112 excitation/emission region had multiple maxima positions (375/472, 360/461, 285/467, 230/418,
113 330/425 and 310/419 nm).
114 Dynamic light scattering examination of the final solution revealed the appearance of large
115 particles (Supplementary Figure 1). There was also a substantial increase in the sample's optical
116 density over the examined wavelength region (Supplementary Figure 2). In a paper by Do *et*
117 *al.*(Do, Kincannon & Bowers, 2015) a theoretical model of the aggregates composed of Phe
118 tetramer units was proposed. These units could interact through π-stacking, creating a fibrillar
119 structure. The newly emerged emission bands would be the result of exciton exchange between

120   aromatic rings. The appearance of longer wavelength emissions following incubation could be
121   the result of J-aggregate-type interactions between these tetramer units, forming larger structures.
122   Surprisingly, the fluorescence region was partially overlapping with the excitation/emission
123   maxima of amyloid-bound ThT(Voropai et al., 2003). This could cause false-positive ThT assay
124   results and give an inaccurate impression of amyloid fibril formation, despite it being π-
125   aggregate assembly.
126   The appearance of optical properties (Figure 2A) could be the result of chemical modifications
127   that occur to Phe upon incubation at 60 °C (Tikhonova et al., 2018). In order to test such a
128   possibility, we attempted to remove the aggregates using filtration through 0.22 μm filters
129   (Figure 2B). We also utilized a 3 kDa concentrator to remove any smaller aggregates (Figure
130   2C), as there were reports indicating that their size could be as low as trimers (Spitz et al., 2002;
131   Kuo, 2011)). The sample was also sonicated to examine the aggregate assembly stability (Figure
132   2D).
133   Filtration through a 0.22 μm filter resulted in a decrease of the six excitation/emission maxima
134   associated with the newly formed aggregates and an increase in Phe-specific band intensity
135   (Table 1). A similar result was achieved after the sample's sonication, however, there was a
136   noticeably larger decrease in intensity at the 375/472 maxima, which could indicate that some
137   smaller aggregates that are able to pass through a 0.22 μm filter can be disassembled. There was
138   also no apparent increase in any of the aggregate-specific maxima, which could mean that all
139   aggregates are affected by sonication, since any larger structure disassembly would lead to an
140   increased band intensity of the smaller assemblies.
141   Filtration through a 3 kDa concentrator yielded a much greater decrease in fluorescence of the
142   aggregate-specific bands and a sizeable increase in Phe-specific band intensity. Interestingly,
143   while the increase in Phe-specific band intensities was similar for all four measured maxima
144   positions, there was a disparity between the remaining six maxima intensity changes. The
145   375/472, 360/461 and 285/467 position intensities decreased significantly, while 230/418,
146   330/425 and 310/419 position intensities experienced a minimal change. This means that the
147   resulting spectra may be composed of both chemically modified Phe (at positions that experience
148   minimal change) and Phe aggregates. It was clear that larger aggregates had specific
149   excitation/emission characteristics and that there was a correlation between the emission
150   intensity increase of Phe-specific maxima positions and the decrease in aggregate-specific
151   maxima positions.
152   After an examination of the excitation/emission properties of the Phe solution spectra we can see
153   that the Phe-specific emission bands overlap with the aggregate-specific excitation wavelengths.
154   Such an overlap could lead to Forster resonance energy transfer (FRET) between non-aggregated
155   Phe molecules, chemically modified Phe and Phe assemblies. Upon a detailed analysis, it seems
156   likely that the Phe-specific emissions can be absorbed by either aggregates or modified Phe and
157   lead to an emission maximum at 230/418. The 230/418 FRET emissions could be caused by Phe
158   molecules and 330/425 and 310/419 bands which are related to smaller assemblies or modified
159   Phe and these FRET emissions experience almost no reduction in intensity upon filtration or

160   sonication. The 285/467 FRET emissions, however, could be related to larger aggregates and
161   diminish greatly upon filtration or sonication. The FRET hypothesis could explain why the
162   removal of aggregates causes an increase of Phe-specific fluorescence.
163   A hydrogel fluorescence assay was also conducted to check whether the previously reported
164   increase in ThT fluorescence intensity upon Phe hydrogel formation was due to ThT
165   immobilization or amyloid formation. Two hydrogels containing ThT were prepared, one using a
166   300 mM Phe solution and another with 1% agarose. Both assays were conducted under the same
167   heating and subsequent cooling conditions and their ThT fluorescence emission spectra were
168   measured during the cooling process.
169   In the case of agarose gel formation (Figure 3A), a fluorescence emission maximum appeared at
170   484 nm and an increase in ThT fluorescence at this maximum increased from 13 ± 2 a.u. to 83 ±
171   2 a.u. (>6-time increase). As for the 300 mM Phe solution (Figure 3B), the emission maximum
172   was at 485 nm and the increase in ThT fluorescence was from 26 ± 10 a.u. to 85 ± 33 a.u. (>3-
173   time increase).
174   With both gels we observe a similar emission maxima position as well as a substantial emission
175   intensity growth. This maxima position correlates with the ones often seen in amyloid fibril
176   staining with ThT(Voropai et al., 2003), however, it is quite obvious that agarose does not form
177   amyloid fibrils, as it is not even an amino acid, which leads to the conclusion that such an
178   emission spectra is the result of ThT immobilization and not binding to amyloid fibril surface.
179   Such a coincidence could easily lead to a false-positive result in detecting amyloid fibril
180   formation.
181   The addition of ThT to the incubated Phe sample (Figure 4A) resulted in a decrease of Phe
182   aggregate-specific emissions (Figure 4B). If the solution contained amyloid fibrils, capable of
183   binding ThT, we would see a noticeable increase in fluorescence emissions at the 440/480
184   excitation/emission region. The observed decrease in the region's fluorescence emission
185   intensity can be explained by the absorption of aggregate-specific emissions by ThT molecules,
186   which in turn do not exhibit fluorescence, due to not being bound to any amyloid fibrils.
187   These results show that in the case of Phe aggregates generated under these conditions, ThT acts
188   as a fluorescence quenching agent and actually hinders the detection of these structures.
189

Conclusions

191   These findings show that Phe does indeed form aggregates, as was demonstrated on multiple
192   occasions, however, autofluorescence of the aggregates, described in this work, partially
193   overlaps with the spectra of dyes used in amyloid fibril assays. Furthermore, the formation of
194   hydrogels can lead to immobilization of ThT and result in an increased emission intensity, which
195   is not the result of interactions with beta-sheet structures.
196

References

198   Adler-Abramovich L., Vaks L., Carny O., Trudler D., Magno A., Caflisch A., Frenkel D., Gazit
199   E. 2012. Phenylalanine assembly into toxic fibrils suggests amyloid etiology in

200   phenylketonuria. *Nature chemical biology* 8:701–6. DOI: 10.1038/nchembio.1002.

201   Anand BG., Dubey K., Shekhawat DS., Kar K. 2017. Intrinsic property of phenylalanine to
202   trigger protein aggregation and hemolysis has a direct relevance to phenylketonuria.
203   *Scientific reports* 7:11146. DOI: 10.1038/s41598-017-10911-z.

204   Azriel R., Gazit E. 2001. Analysis of the minimal amyloid-forming fragment of the islet amyloid
205   polypeptide. An experimental support for the key role of the phenylalanine residue in
206   amyloid formation. *The Journal of biological chemistry* 276:34156–61. DOI:
207   10.1074/jbc.M102883200.

208   Banik D., Dutta R., Banerjee P., Kundu S., Sarkar N. 2016. Inhibition of Fibrillar Assemblies of
209   l-Phenylalanine by Crown Ethers: A Potential Approach toward Phenylketonuria. *The*
210   *journal of physical chemistry. B* 120:7662–70. DOI: 10.1021/acs.jpcb.6b05209.

211   Banik D., Kundu S., Banerjee P., Dutta R., Sarkar N. 2017. Investigation of Fibril Forming
212   Mechanisms of l-Phenylalanine and l-Tyrosine: Microscopic Insight toward
213   Phenylketonuria and Tyrosinemia Type II. *The journal of physical chemistry. B* 121:1533–
214   1543. DOI: 10.1021/acs.jpcb.6b12220.

215   von Bergen M., Friedhoff P., Biernat J., Heberle J., Mandelkow E-M., Mandelkow E. 2000.
216   Assembly of tau protein into Alzheimer paired helical filaments depends on a local
217   sequence motif (306VQIVYK311) forming beta structure. *Proceedings of the National*
218   *Academy of Sciences* 97:5129–5134. DOI: 10.1073/pnas.97.10.5129.

219   Cao X., Meng L., Li Z., Mao Y., Lan H., Chen L., Fan Y., Yi T. 2014. Large red-shifted
220   fluorescent emission via intermolecular π-π stacking in 4-ethynyl-1,8-naphthalimide-based
221   supramolecular assemblies. *Langmuir: the ACS journal of surfaces and colloids* 30:11753–
222   60. DOI: 10.1021/la503299j.

223   Chiti F., Dobson CM. 2006. Protein Misfolding, Functional Amyloid, and Human Disease.
224   *Annual Review of Biochemistry* 75:333–366. DOI:
225   10.1146/annurev.biochem.75.101304.123901.

226   Do TD., Kincannon WM., Bowers MT. 2015. Phenylalanine Oligomers and Fibrils: The
227   Mechanism of Assembly and the Importance of Tetramers and Counterions. *Journal of the*
228   *American Chemical Society* 137:10080–3. DOI: 10.1021/jacs.5b05482.

229   Fitzpatrick AWP., Debelouchina GT., Bayro MJ., Clare DK., Caporini MA., Bajaj VS., Jaroniec
230   CP., Wang L., Ladizhansky V., Muller SA., MacPhee CE., Waudby CA., Mott HR., De
231   Simone A., Knowles TPJ., Saibil HR., Vendruscolo M., Orlova E V., Griffin RG., Dobson
232   CM. 2013. Atomic structure and hierarchical assembly of a cross- amyloid fibril.
233   *Proceedings of the National Academy of Sciences* 110:5468–5473. DOI:
234   10.1073/pnas.1219476110.

235   Gazit E. 2002. A possible role for pi-stacking in the self-assembly of amyloid fibrils. *FASEB*
236   *journal: official publication of the Federation of American Societies for Experimental*
237   *Biology* 16:77–83. DOI: 10.1096/fj.01-0442hyp.

238   Gazit E. 2007. Self assembly of short aromatic peptides into amyloid fibrils and related
239   nanostructures. *Prion* 1:32–35. DOI: 10.4161/pri.1.1.4095.

240   German HW., Uyaver S., Hansmann UHE. 2015. Self-assembly of phenylalanine-based
241   molecules. *The journal of physical chemistry. A* 119:1609–15. DOI: 10.1021/jp5077388.

242   Griffith EC., Perkins RJ., Telesford D-M., Adams EM., Cwiklik L., Allen HC., Roeselová M.,
243   Vaida V. 2015. Interaction of L-Phenylalanine with a Phospholipid Monolayer at the Water-
244   Air Interface. *The journal of physical chemistry. B* 119:9038–48. DOI: 10.1021/jp508473w.

245   Halverson K., Fraser PE., Kirschner DA., Lansbury PT. 1990. Molecular determinants of

246   amyloid deposition in Alzheimer's disease: conformational studies of synthetic .beta.-
247   protein fragments. *Biochemistry* 29:2639–2644. DOI: 10.1021/bi00463a003.
248   Handelman A., Kuritz N., Natan A., Rosenman G. 2016. Reconstructive Phase Transition in
249   Ultrashort Peptide Nanostructures and Induced Visible Photoluminescence. *Langmuir: the*
250   *ACS journal of surfaces and colloids* 32:2847–62. DOI: 10.1021/acs.langmuir.5b02784.
251   Higgins DA., Barbara PF. 1995. Excitonic transitions in J-aggregates probed by near-field
252   scanning optical microscopy. *The Journal of Physical Chemistry* 99:3–7. DOI:
253   10.1021/j100001a002.
254   Hutter T., Amdursky N., Gepshtein R., Elliott SR., Huppert D. 2011. Study of thioflavin-T
255   immobilized in porous silicon and the effect of different organic vapors on the fluorescence
256   lifetime. *Langmuir: the ACS journal of surfaces and colloids* 27:7587–94. DOI:
257   10.1021/la200875k.
258   Kuo A. 2011. Fluorescence Resulting from π-stacking in Polystyrene Solutions. *CheM* 1:80–86.
259   DOI: 10.5618/chem.2011.v1.n1.9.
260   De Luigi A., Mariani A., De Paola M., Re Depaolini A., Colombo L., Russo L., Rondelli V.,
261   Brocca P., Adler-Abramovich L., Gazit E., Del Favero E., Cantù L., Salmona M. 2015.
262   Doxycycline hinders phenylalanine fibril assemblies revealing a potential novel therapeutic
263   approach in phenylketonuria. *Scientific reports* 5:15902. DOI: 10.1038/srep15902.
264   McRae EG., Kasha M. 1958. Enhancement of Phosphorescence Ability upon Aggregation of
265   Dye Molecules. *The Journal of Chemical Physics* 28:721–722. DOI: 10.1063/1.1744225.
266   Mossou E., Teixeira SCM., Mitchell EP., Mason SA., Adler-Abramovich L., Gazit E., Forsyth
267   VT. 2014. The self-assembling zwitterionic form of L-phenylalanine at neutral pH. *Acta*
268   *crystallographica. Section C, Structural chemistry* 70:326–31. DOI:
269   10.1107/S2053229614002563.
270   Perween S., Chandanshive B., Kotamarthi HC., Khushalani D. 2013. Single amino acid based
271   self-assembled structure. *Soft Matter* 9:10141. DOI: 10.1039/c3sm51054a.
272   Reches M., Gazit E. 2003. Casting metal nanowires within discrete self-assembled peptide
273   nanotubes. *Science (New York, N.Y.)* 300:625–7. DOI: 10.1126/science.1082387.
274   Shaham-Niv S., Adler-Abramovich L., Schnaider L., Gazit E. 2015. Extension of the generic
275   amyloid hypothesis to nonproteinaceous metabolite assemblies. *Science advances*
276   1:e1500137. DOI: 10.1126/sciadv.1500137.
277   Singh V., Rai RK., Arora A., Sinha N., Thakur AK. 2014. Therapeutic implication of L-
278   phenylalanine aggregation mechanism and its modulation by D-phenylalanine in
279   phenylketonuria. *Scientific reports* 4:3875. DOI: 10.1038/srep03875.
280   Smith AM., Williams RJ., Tang C., Coppo P., Collins RF., Turner ML., Saiani A., Ulijn R V.
281   2008. Fmoc-Diphenylalanine Self Assembles to a Hydrogel via a Novel Architecture Based
282   on π–π Interlocked β-Sheets. *Advanced Materials* 20:37–41. DOI:
283   10.1002/adma.200701221.
284   Spitz C., Knoester J., Ouart A., Daehne S. 2002. Polarized absorption and anomalous
285   temperature dependence of fluorescence depolarization in cylindrical J-aggregates.
286   *Chemical Physics* 275:271–284. DOI: 10.1016/S0301-0104(01)00521-3.
287   Tikhonova TN., Rovnyagina NR., Zherebker AY., Sluchanko NN., Rubekina AA., Orekhov AS.,
288   Nikolaev EN., Fadeev V V., Uversky VN., Shirshin EA. 2018. Dissection of the deep-blue
289   autofluorescence changes accompanying amyloid fibrillation. *Archives of Biochemistry and*
290   *Biophysics* 651:13–20. DOI: 10.1016/j.abb.2018.05.019.
291   Uemori Y., Munakata H., Kitazawa S., Osada A., Imai H. 2012. Optically active J-aggregate

292   formed from water-soluble porphyrin with phenylalanine. *Journal of Porphyrins and*
293   *Phthalocyanines* 16:1285–1292. DOI: 10.1142/S1088424612501441.
294 Voropai ES., Samtsov MP., Kaplevskii KN., Maskevich AA., Stepuro VI., Povarova OI.,
295   Kuznetsova IM., Turoverov KK., Fink AL., Uverskii VN. 2003. Spectral Properties of
296   Thioflavin T and Its Complexes with Amyloid Fibrils. *Journal of Applied Spectroscopy*
297   70:868–874. DOI: 10.1023/B:JAPS.0000016303.37573.7e.
298

Figure 1

Excitation/emission spectra of 100 mM L-phenylalanine measured every 3 days during a 15-day incubation period.

The examined spectra region contains a 2nd order diffraction artefact of Phe (marked in the no incubation spectra). 5 nm excitation and emission slits were used.
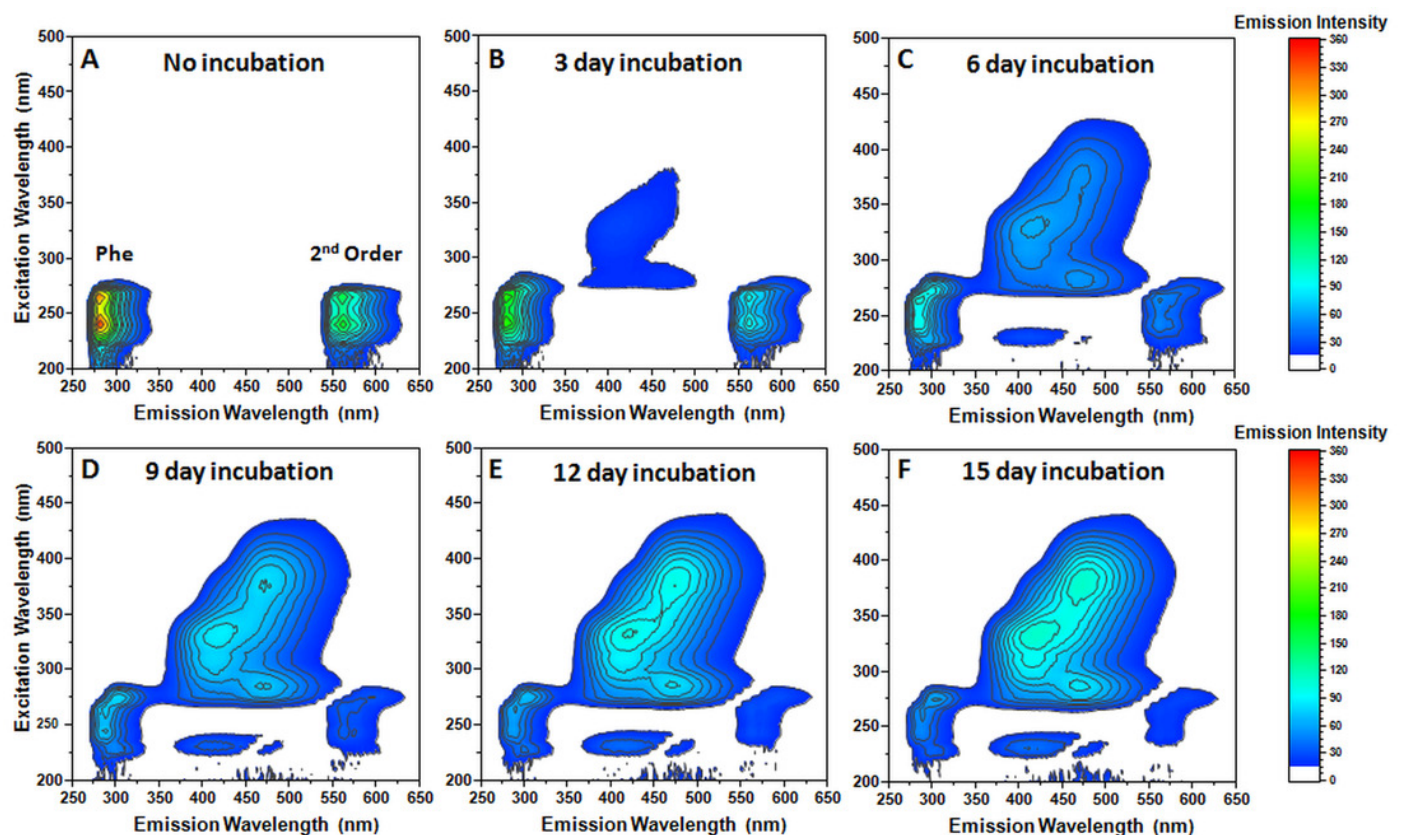
Figure 2

Effect of filtration and sonication on the spectra of aggregated Phe.

10 nm excitation and 5 nm emission slits were used.
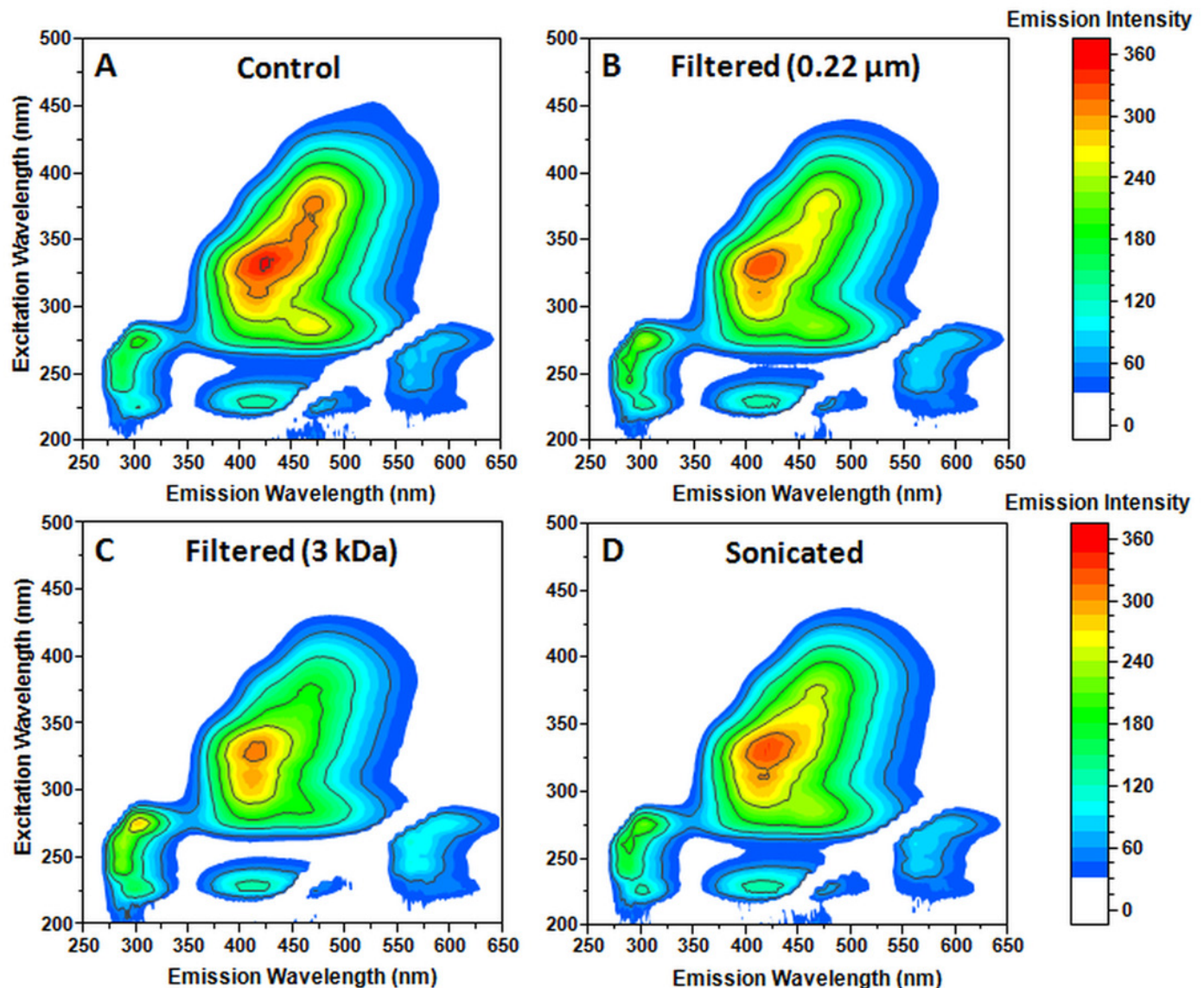
Figure 3

1% agarose and 300 mM Phe gel formation induced ThT fluorescence emission changes (sample excitation wavelength – 440 nm).

10 nm excitation and 5 nm emission slits were used. Emission intensity was calculated from

3 separate measurements.
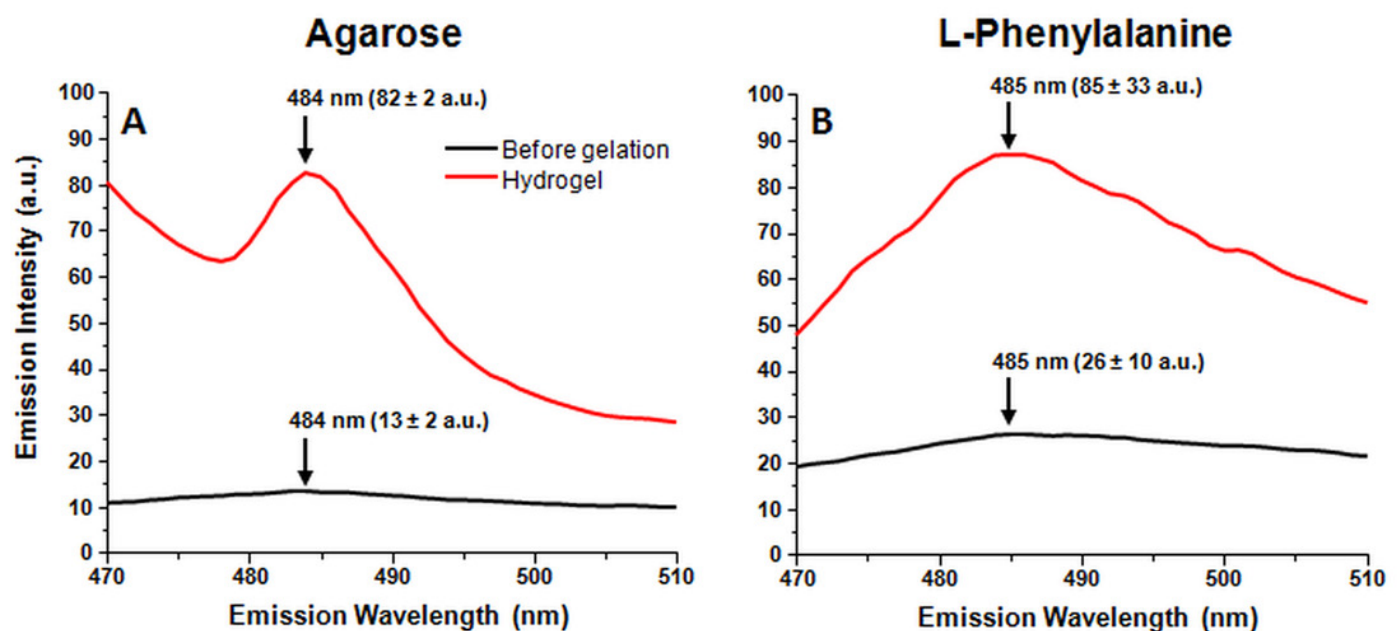
Figure 4

Aggregated Phe fluorescence emission changes after the addition of 50 μM ThT.

10 nm excitation and 5 nm emission slits were used.
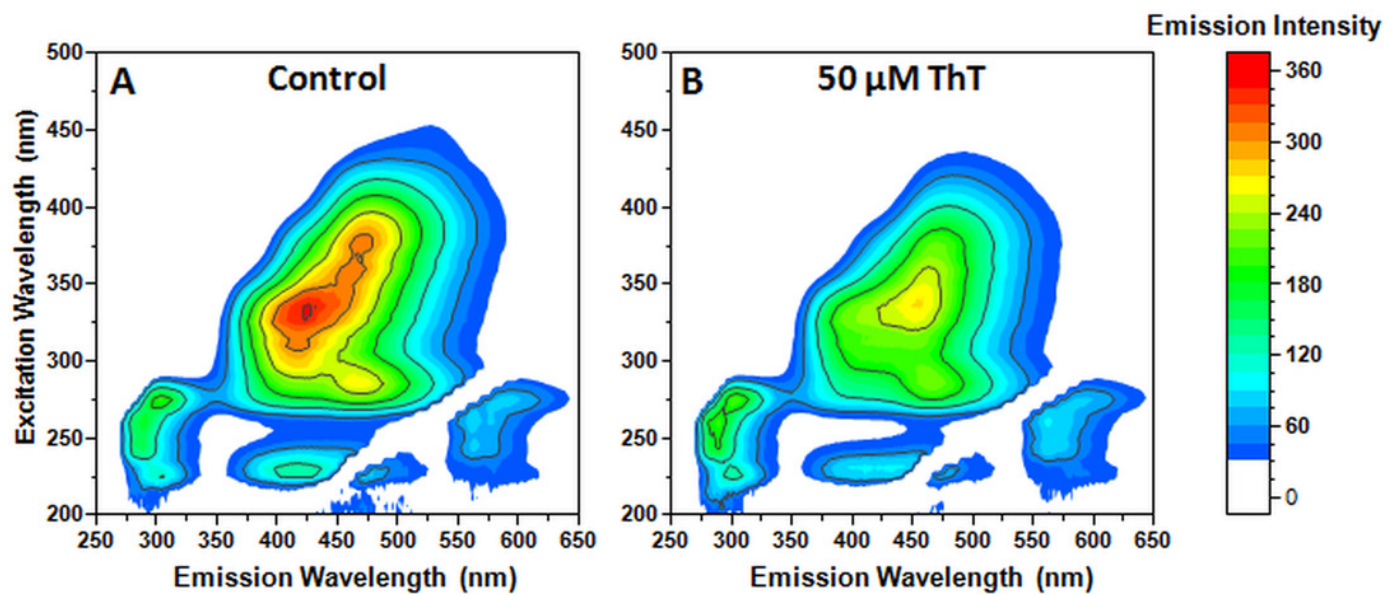
Fluorescence emission intensity changes of Phe-specific, aggregate-specific, and FRET maxima.

Filtration- and sonication- induced fluorescence emission intensity changes for Phe-specific (green), aggregate-specific (red) and FRET (blue) maxima.

Excitation	Emission	Control Intensity	Filtered (0.22 μm) Intensity	Change (%)	Filtered (3 kDa) Intensity	Change (%)	Sonicated Intensity	Change (%)
275	303	204 ± 3	241 ± 17	18 ± 7	285 ± 21	40 ± 8	219 ± 2	8 ± 2
260	290	180 ± 2	202 ± 11	13 ± 6	240 ± 20	33 ± 8	197 ± 2	9 ± 1
245	288	163 ± 4	187 ± 11	15 ± 6	223 ± 20	37 ± 9	179 ± 2	10 ± 3
225	304	127 ± 7	142 ± 7	12 ± 8	170 ± 16	34 ± 11	137 ± 4	8 ± 6
375	472	312 ± 1	266 ± 7	-15 ± 3	187 ± 22	-40 ± 12	248 ± 3	-21 ± 1
360	461	311 ± 1	266 ± 11	-14 ± 4	203 ± 20	-35 ± 10	267 ± 2	-14 ± 1
330	425	347 ± 6	324 ± 7	-7 ± 3	303 ± 15	-13 ± 5	330 ± 2	-5 ± 2
310	419	310 ± 3	297 ± 6	-4 ± 2	294 ± 8	-5 ± 3	304 ± 1	-2 ± 1
285	467	270 ± 3	232 ± 6	-14 ± 3	187 ± 13	-31 ± 6	239 ± 1	-11 ± 1
230	418	139 ± 2	134 ± 3	-3 ± 3	138 ± 2	-1 ± 2	137 ± 2	-1 ± 2